Comparison of Algorithms to Calculate Plume Centerline Temperature and Ceiling Jet Temperature with Experiments

WILLIAM D. DAVIS*

National Institute of Standards and Technology, 100 Bureau Dr. STOP 8642, Gaithersburg, MD 20899 8642, USA

ABSTRACT: The predictive capability of two algorithms designed to calculate plume centerline temperature and maximum ceiling jet temperature in the presence of a hot upper layer are compared to measurements from experiments that developed a hot layer. In addition, comparisons are made using the ceiling jet algorithm in CFAST (Version 3.1). The experiments include ceiling heights of 0.58 m to 22 m and heat release rates (HRR) of 0.62 kW to 33 MW. With the combined uncertainty of the measurement and the calculation roughly equal to ±20%, the algorithms of Evans and Davis consistently provided predictions either close to or within this uncertainty interval for all fire sizes and ceiling heights while the ceiling jet algorithm in CFAST consistently over-predicted the temperature.

KEY WORDS: ceiling jets, fire experiments, fire models, fire plumes, temperature correlations, temperature measurements.

INTRODUCTION

RECENT EXPERIMENTS [1] have highlighted the need for an improved predictive capability for both ceiling jet temperature and plume centerline temperature in draft curtained, high bay spaces when upper layers develop. Algorithms have been developed and tested using JET [2], a modified version of the zone fire model LAVENT [3], that are able to simulate plume centerline temperature and ceiling jet temperature for the experiments [1]. These algorithms have subsequently been included in CFAST (Version 3.1) [4] in order to test their accuracy using this platform. This study compares the predictions of the algorithms for ceiling jet

*E-mail: williamdavis@nist.gov

1042-3915/02/01 0009–21 $10.00/0 DOI: 10.1106/104239102022850

temperature [2] and plume centerline temperature [5] with the measurements by various investigators [1,6–9]. Also included in the comparisons are the ceiling jet predictions of CFAST (Version 3.1) [10].

The experiments selected for comparison with these models span a wide range of parameters including ceiling height and fire size. Since this work is done in the context of buildings, only experiments that formed a hot ceiling layer are used. In most instances, comparison between prediction and measurement is made after the growing fire has reached a steady-state heat release rate (HRR). Plume centerline temperature comparisons are made for ceiling heights ranging from 0.58 m to 22 m while ceiling jet temperature comparisons are made for ceiling heights ranging from 1 m to 22 m.

THEORY

Plume Centerline Temperature

The analysis of fire plumes is based on the solution of the conservation laws for mass, momentum and energy. Early work centered on point sources and assumed that the air entrainment velocity at the edge of the plume was proportional to the local vertical plume velocity [11]. Measurements of plume centerline temperature in plumes with unconfined ceilings led to a correlation developed by Heskestad [12] that was consistent with theory. The correlation gives the excess temperature as a function of height above a virtual point source to be

$$\Delta T_p = 9.1\left(\frac{T_\infty}{g\, c_p^2\, \rho_\infty^2}\right)^{1/3} Q_c^{\,2/3}(z - z_0)^{-5/3} \tag{1}$$

The virtual origin (z_0) is given by

$$z_0 = -1.02D + 0.083\, Q^{2/5} \tag{2}$$

where Q and Q_c are the total and convective heat release rates, respectively, D is the fire diameter, z is the height above the fire surface, and T_∞, c_p, and ρ_∞ are the temperature, heat capacity, and density of the ambient gas, respectively. When a hot upper layer forms, this correlation must be modified in order to predict plume centerline temperature since the plume now includes added enthalpy by entraining hot layer gas as it moves through the upper layer to the ceiling. Methods of defining a substitute virtual source and HRR in order to extend the plume into the upper layer have been developed by Cooper [13] and Evans [5]. Evans' method defines the strength

$Q_{I,2}$ and location $Z_{I,2}$ of the substitute source with respect to the interface between the upper and lower layers by

$$Q^*_{I,2} = [(1 + C_T\, Q^{*2/3}_{I,1})/\xi C_T - 1/C_T]^{3/2} \tag{3}$$

$$Z_{I,2} = \left[\frac{\xi\, Q^*_{I,1}\, C_T}{Q^{*1/3}_{I,2}\left[(\xi - 1)(\beta^2 + 1) + \xi C_T Q^{*2/3}_{I,2}\right]}\right]^{2/5} Z_{I,1} \tag{4}$$

$$Q^*_{I,1} = Q_c\,/(\rho_\infty C_\infty T_\infty g^{1/2} Z^{5/2}_{I,1}) \tag{5}$$

where $Z_{I,1}$ is the distance from the fire to the interface between the upper and lower layer, ξ is the ratio of upper to lower layer temperature, β is an experimentally determined constant [14] ($\beta^2 = 0.913$) and $C_T = 9.115$. The distance between the virtual source and the ceiling, H_2, is then obtained from

$$H_2 = H_1 - Z_{I,1} + Z_{I,2} \tag{6}$$

where H_1 is the location of the fire beneath the ceiling (see Figure 1). The new values of the fire source and ceiling height are then used in a standard plume correlation [15] where the ambient temperature is now the temperature of the upper layer (the two layer environment has been replaced by

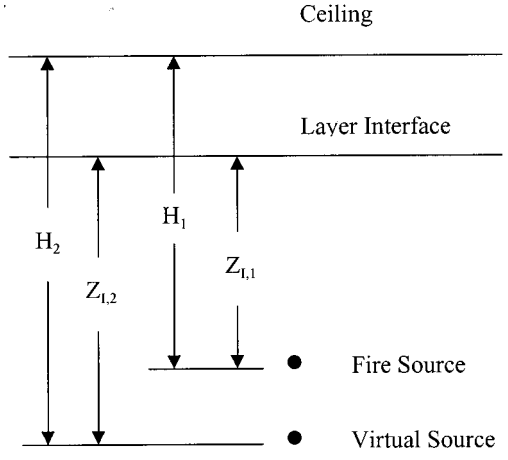

Figure 1. *Graphical representation of the relationship between the fire source ($Q_{I,1}$) and the virtual source ($Q_{I,2}$).*

a single layer with a temperature equal to the upper layer temperature). The plume excess temperature is given by

$$\Delta T_p = 9.28 T_u (\mathrm{Q}^*_{I,2})^{2/3} \left(\frac{Z_{I,2}}{H_2} \right)^{5/3} \tag{7}$$

where T_u is the temperature of the upper layer.

Ceiling Jet Algorithm

The ceiling jet temperature algorithm [2] predicts the maximum temperature excess of the ceiling jet in the presence of a growing upper layer. The ceiling jet temperature excess as a function of radius for $r/H > 0.18$ is given by

$$\Delta T = k \Delta T_p \left(\frac{r_o}{r} \right)^{\gamma} \tag{8}$$

$$k = (0.68 + 0.16(1 - e^{-y_L/y_J})) \tag{9}$$

$$r_0 = 0.18H \tag{10}$$

where

$$\gamma = 2/3 - \alpha(1 - e^{-y_L/y_J}) \tag{11}$$

and $\alpha = 0.44$, $y_J = 0.1 \times H$, y_L is the layer thickness, and ΔT_p is the plume centerline temperature excess as calculated using Evans' method (Equations (3)–(7)). When a hot layer is not present, the model reduces to the correlation of Alpert [16] for $r/H > 0.18$ with the exception that the convective heat release rate (HRR_c) rather than the total heat release is used in the correlation.

A short explanation of the basis for this algorithm will be given since the algorithm has not appeared in the journal literature. The algorithm was developed using experiments by Gott [1] that were JP-5 and JP-8 pan fires conducted in hangars of ceiling heights 15 m and 22 m. The 15 m hangar had an almost flat ceiling while the 22 m hangar had a ceiling that could be described as barrel shaped. The ceiling in the 22 m hangar in the direction of the barrel ceiling was fairly flat for the first 12 m from the plume centerline and then began to curve downward with an increasing loss of height.

The evolution of the radial temperature dependence of the ceiling jet in time is given in Figure 2 for the 2.8 MW JP-5 pan fire in the 22 m hangar

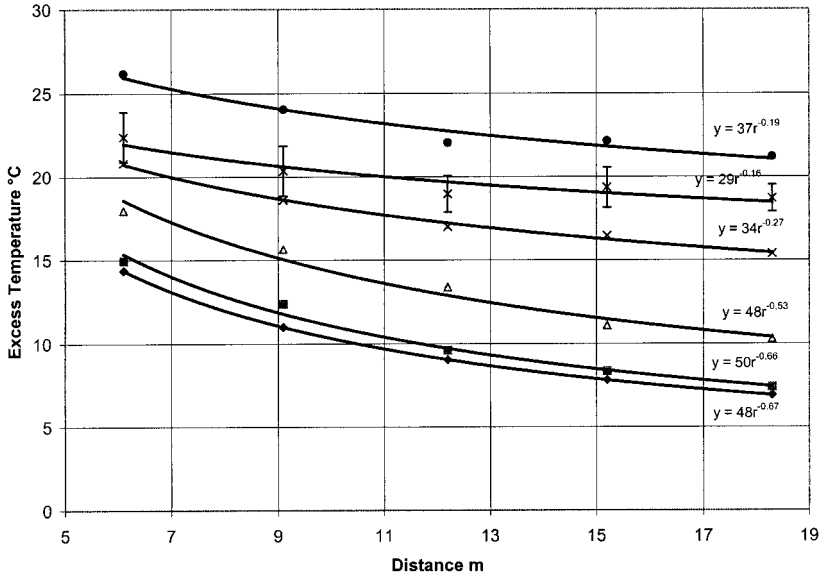

Figure 2. *Time evolution of the radial temperature dependence of the ceiling jet for the 2.8 MW JP-5 pan fire at a ceiling height of 22 m. The measurements are averaged on the east and west sides of plume center in the direction of the barrel roof. The lowest curve is Alpert's correlation evaluated using the 2.8 MW heat release rate. The next five curves from bottom to top represent the ceiling jet temperature at times of 80 s, 100 s, 150 s, 200 s, and 300 s. Power law curve fits are given for each data set and Alpert's correlation as a function of distance, r, from plume center. Uncertainty intervals shown for the measured values are one sigma intervals based on a least squares average of five data points taken during a twenty second interval.*

(see Reference [17] for additional details). The measurements were made in the direction of the barrel ceiling. The temperature values are based on an average of five data points centered on the given time with a one-sigma uncertainty shown on one of the curves. The average time between data points is 4.0 s. Also shown in the figure is the ceiling jet temperature predicted by Alpert's correlation for unconfined ceilings [16]. Early in the experiment, before a layer has had time to form, the measured ceiling jet temperature corresponds to Alpert's correlation. The good agreement between the measurements and this correlation suggests that the curvature of the roof has only a minor impact on the temperature dependence of the ceiling jet.

As the hot layer develops, the ceiling jet temperature increases and the radial dependence of the temperature decreases. The reason for the change in the radial dependence from that predicted by Alpert's correlation is that, as a hot upper layer develops, the ceiling jet begins to entrain hot air rather

than cooler ambient air. The depth of the layer will determine how much of the ambient air is entrained in addition to the hot upper layer air. The data presented in Figures 3 and 4 provides additional evidence for the changing radial temperature dependence as a hot layer develops for heights of 15 m and 22 m. Similar results were observed by Motevalli and Ricciuti [7] in their 1.0 m reduced scale experiment and by Zukowski and Kubota in a hood experiment [18].

Since the draft curtains were of different depths in the two hangars, the experiments provided guidance in determining how the layer depth affected the radial temperature dependence. The radial dependence of the temperature, γ, would change from Alpert's value of 0.67 for an unconfined ceiling to a value of 0.23 ± 0.07 as a hot layer developed. Based on these values, the value for $\alpha = 0.44$ was determined.

The value for k was developed using the ratio of the plume centerline temperature to the temperature at the start of the ceiling jet. With no hot layer, $k = 0.67 \pm 0.11$ and as the hot layer developed the value of k was observed to increase to 0.84 ± 0.04. This effect stems from the decreasing entrainment of ambient air at the edge of the plume as the hot layer forms.

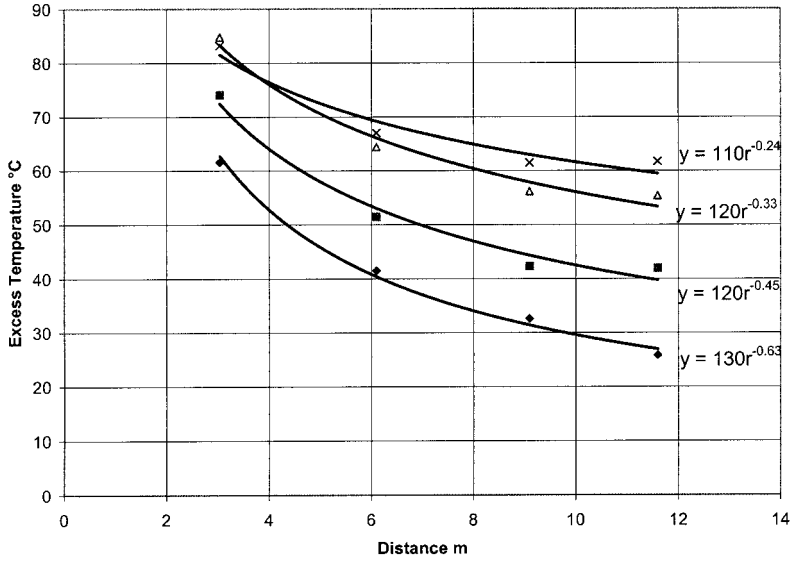

Figure 3. *Time evolution of the radial temperature dependence of the ceiling jet for the 7.7 MW JP-5 pan fire with draft curtain at a 15 m high ceiling. The four curves correspond to experimental times of 70 s, 100 s, 200 s, and 300 s from bottom to top respectively.*

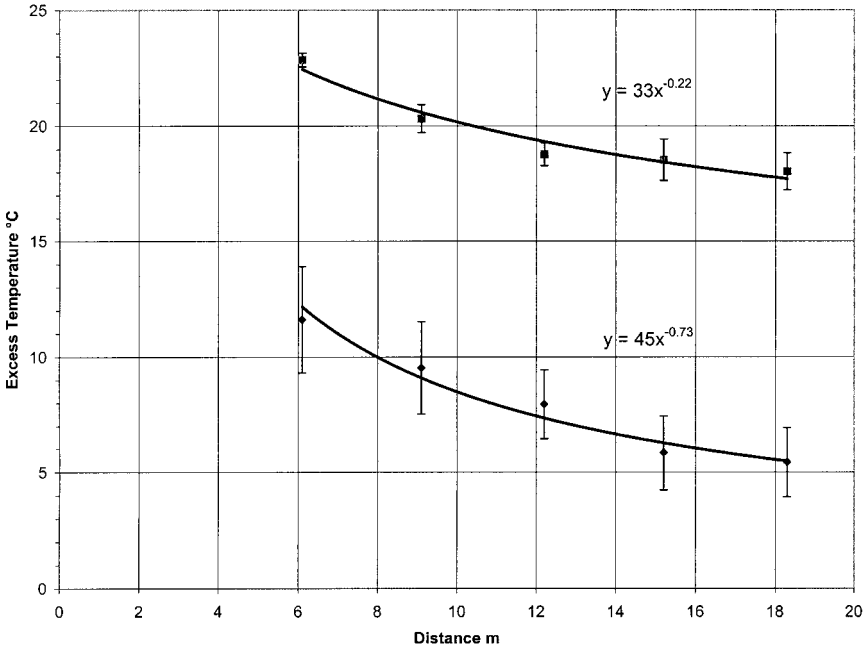

Figure 4. *Averaged ceiling jet temperature for the 2.8 MW, 4.9 MW, 7.9 MW, 14.6 MW and 15.7 MW tests at a ceiling height of 22 m. The bottom curve represents the ceiling jet with no layer while the top curve represents the ceiling jet at 200 s after a layer has filled the draft curtains. Temperatures are scaled to the convective heat release rate of the 2.8 MW test. Uncertainty intervals shown on the figure represent the one-sigma interval deduced from averaging the scaled temperatures at each point from the five tests.*

The parameter y_J was originally given a value of 1.0 m [17] based on the assumption that radiation was a major reason why the ceiling jet was cooling off. When the algorithm was compared to Motevalli's [7] reduced-scale experiment with a 1.0 m ceiling height, it became clear that the original value was incorrect. The scale height $0.1 \times H$, which is the approximate thickness of the ceiling jet, was substituted for the 1.0 m value based on the assumption that the entrainment of ambient air by the ceiling jet may be related to both the thickness of the ceiling jet and the thickness of the upper layer.

COMPARISON OF MODEL PREDICTIONS WITH EXPERIMENTS

Data from a series of experiments was obtained for comparison with the predictions of the algorithms described above. A brief description of each experiment will be included in the sections below. The experiments will be organized according to the distance between the fire source and the ceiling

with the range being 0.58 m to 22 m. Upper layer temperature excess will be given when available and compared to the calculated value. The new algorithms for ceiling jet temperature and plume centerline temperature using CFAST as the computational base will be designated as DNT in the comparisons, while the present ceiling jet algorithm in CFAST, Version 3.1 will be designated as v3.1.

Uncertainty intervals are provided for both experimental measurements and model predictions. For each experiment, the experimental uncertainties are either those given in the report or are estimated based on the experimental data and fire type. The uncertainty intervals are shown in Tables 1–6 as a split row to the right of the column containing the measured or calculated value.

Computer fire models require a number of experimentally determined input values and the uncertainty in each input value generates an uncertainty in the calculated result. Uncertainty intervals for the models in this paper are based on the estimated uncertainty in the HRR_c for each experiment. Uncertainties in the measurement of the distance between the fire and the ceiling, and the material properties of the walls and ceiling are neglected. The uncertainty in HRR_c is equal to the combined uncertainty for the HRR and the radiative fraction. For those experiments where these uncertainties were not available from the paper, the uncertainties represent a best guess based on the type of fire and fuel type used in the experiment. The uncertainty intervals for the calculations were obtained by using a high, middle and low estimate of the HRR_c since changing the HRR will impact the layer temperature. The estimates were done either by varying the radiative fraction or by varying the total HRR. Since the HRR_c, is given by

$$\mathrm{HRR}_c = (1 - \chi_r)\mathrm{HRR} \tag{12}$$

varying either the radiative fraction, χ_r, or the HRR will have the same effect on HRR_c.

Predictions and measurements are judged to be in agreement when the uncertainty intervals overlap. While it is tempting to compare the measured and predicted values and ignore the uncertainty intervals, the uncertainty intervals are a guide to the accuracy of a measurement or model prediction.

Evans (Ceiling Height of 0.58 m)

A cylindrical enclosure of 1.22 m diameter formed by a 0.29 m deep PMMA curtain around a 13 mm thick ceramic fiberboard ceiling was used

to study the temperature produced by an axisymmetric plume. The fire source was a methane gas burner of diameter 0.0365 m located at the center of the cylinder. The top of the burner was located 0.58 m beneath the ceiling. The HRR was 0.62 kW. Details of this experiment are available in Reference [6].

In modeling the experiment, the cylindrical enclosure was approximated by a square enclosure 1.04 m on a side with a 0.29 m deep draft curtain. The ceiling material was approximated using the "sheathing" selection from the CFAST database. The fire was centered in the square at a distance of 0.58 m from the ceiling. The radiation fraction for methane was 0.16.

This experiment measured plume centerline temperature as a function of height but not ceiling jet temperature. The predicted plume centerline temperature excess using DNT is 68°C compared to the measured steady-state value of 60 ± 5°C (Table 1). Uncertainty intervals for the measurements were given in the reference while the uncertainty in the calculations are based on an estimation of the uncertainty in the HRR of the experiment of $\pm 5\%$ and yield a range between 65°C and 70°C. The calculated upper layer excess temperature was 35°C while the measured value was 30°C. The plume centerline temperature excess predicted using DNT lies just within the combined uncertainty interval of the measurement and the calculation.

Motevalli and Ricciuti (Ceiling Height of 1.0 m)

A cylindrical enclosure of diameter 2.13 m formed by a 0.5 m deep corrugated cardboard curtain around a 1.27 cm thick fiberboard ceiling was used to study the development of a ceiling jet at distances of $r/H = 0.26$ and $r/H = 0.75$ where r is the radial distance from the fire center and H is the distance between the burner outlet and the ceiling. The fire consisted of a methane flame produced using a 2.7 cm diameter burner. The burner outlet was located at the center of the cylindrical enclosure and was 1.0 m below the ceiling. The fire sizes used in this study were 0.75 kW and 2.0 kW. Additional details concerning this experiment can be found in Reference [7].

In modeling the experiment, the cylindrical enclosure was approximated by a square enclosure 1.89 m on a side with a 0.50 m deep draft curtain. The ceiling material was approximated using the "sheathing" selection from the CFAST database. The fire was centered in the square at a distance of 1.0 m from the ceiling.

Table 2 presents the predictions of DNT and CFAST (v3.1) with the ceiling jet temperature maximums measured at 300 s. These experiments were conducted for 35 min but the ceiling jet temperature remains nearly constant after 300 s. There was no guidance given by the authors concerning

Table 1. Plume centerline temperature comparison [1,6,9].

Experiment	Measured (°C)		DNT (°C)	
Evans, 0.58 m	60	65 55	68	70 65
Hinkley et al., 10 m	130	134 126	163	179 152
Gott et al., 15 m, 0.48 MW	14	15 13	16	18 15
Gott et al., 15 m, 2.7 MW	46	48 44	52	57 47
Gott et al., 15 m, 7.7 MW	102	106 98	123	137 109
Gott et al., 22 m, 1.4 MW	13	14 12	16	18 14
Gott et al., 22 m, 1.7 MW	15	16 14	18	20 16
Gott et al., 22 m, 2.8 MW	30	32 28	29	32 26
Gott et al., 22 m, 4.9 MW	45	46 44	50	55 44
Gott et al., 22 m, 7.9 MW	67	73 61	75	83 66
Gott et al., 22 m, 14.3 MW	108	120 96	123	135 110
Gott et al., 22 m, 14.6 MW	116	130 102	126	139 111
Gott et al., 22 m, 15.7 MW	115	123 107	132	146 116
Gott et al., 22 m, 33 MW	220	241 199	225	249 197

Table 2. Montevalli 1.0 m ceiling height experiments [7].

Fire Size kW	*r*/*H*	Measured (°C)		DNT (°C)		V 3.1 (°C)	
0.75	0.25	28	31 25	24	26 22	34	37 31
	0.75	19	21 17	19	21 17	28	31 25
2.0	0.25	56	62 50	46	51 41	67	74 60
	0.75	43	47 39	36	40 32	59	65 53

the uncertainties of their measurements. It was assumed that an uncertainty interval of $\pm 10\%$ would be a reasonable approximation of the measurement accuracy that would include systematic errors and data scatter in the temperature measurements. An uncertainty interval of $\pm 10\%$ was also used for the HRR that would include the uncertainties in the burner flow rates, combustion efficiency, and radiative fraction of the fuel source. DNT predicted the ceiling jet temperature within the combined uncertainties of the calculations and the measurements although the trend for both fire sizes was to under predict the temperature. The algorithm in Version 3.1 of CFAST predicted the ceiling jet temperature at $r/H = 0.26$ within the combined uncertainties but over-predicted the temperature at $r/H = 0.75$. CFAST calculated the upper layer excess temperature to be 17°C and 37°C for the 0.75 kW and 2.0 kW experiments while the measured values were 14 and 31°C, respectively.

Heskestad and Delichatsios (Ceiling Height of 2.7 m)

A series of experiments was conducted using a ceiling measuring 9.75 m × 14.6 m. Simulated beams, 0.305 m deep and separated by 1.22 m, were installed on the ceiling with the beams parallel to the long dimension of the ceiling. A pair of experiments (Tests 7 and 4), one with a 1.22 m deep draft curtain and one without a draft curtain, was chosen for the analysis. Wood cribs were used as the fire source with the bottom of the beams located 2.43 m above the top of the wood cribs. This pair of tests was chosen out of a set of three test pairs based on similar moisture content of the wood and nearly identical *t*-squared fire growth rates. Since the growth rate of the fire as a function of time was provided, comparisons were made at several different fire sizes. The fire sizes for these comparisons ranged from 30 kW to 830 kW. Additional information concerning the experiments can be found in Reference [8].

In modeling this experiment, the enclosure was rectangular of dimensions 9.75 m × 14.63 m with a ceiling height of 2.74 m. The beams were modeled assuming that a draft curtain 0.305 m deep was attached to the 14.63 m sides of the rectangular ceiling. The draft curtain was modeled by enclosing the rectangular ceiling area by a 1.22 m deep draft curtain. The ceiling was approximated as "gypsum" from the CFAST database. Fire sizes for the draft curtain case were 30.6, 124, 283, 504 and 790 kW while the case without a draft curtain were 32.3, 132, 299, 534, 835 kW at times of 49, 99, 149, 199 and 249 s. The fire was positioned at an *x*–*y* location of 2.15 m and 1.65 m.

Table 3 displays the comparison between DNT and the measurements for the plume centerline temperature for Test 4 which contained 0.305 m deep

Table 3. Heskestad and Delichatsios [8] 2.7 m experiments.

Time (s)	Measured (°C)		DNT (°C)	
Test 4, beams but no draft curtain				
49	49	51	38	43
		47		36
99	109	114	100	112
		104		94
149	211	222	174	195
		200		158
199	378	396	259	291
		360		243
249	450	472	352	396
		428		330
Test 7, beams and draft curtain				
49	52	54	37	41
		50		34
99	118	124	101	113
		112		94
149	242	254	193	220
		230		180
199	482	506	306	348
		458		285

beams and Test 7 which included the ceiling beams plus a 1.22 m deep draft curtain. The uncertainty intervals used for the data are estimated to be $\pm 5\%$ while the calculations were done by taking the reported time dependent HRR and varying the radiative fraction between 0.20 and 0.45. The temperatures are calculated using a radiative fraction of 0.35. As the fire size increases and the layer develops, the predictions of DNT significantly under-predict the plume centerline temperatures.

Several reasons may combine to produce the significant under-prediction at the largest fire sizes for these experiments. First, the combustion region of the flame is approaching the ceiling for the larger fires. The plume algorithms used in these comparisons are valid only out of the combustion region and hence when the flames get close to the ceiling, the accuracy of the plume algorithm comes into question. Second, since the combustion region is close to the ceiling, the radiation to the ceiling and hence to the thermocouple becomes significant. The thermocouple reading would require correction for radiation effects that would effectively lower the measured temperature. This was not done in the experiments. Third, as the fire size increases, the radiative fraction may decrease with fire size as

the fire volume becomes optically thick. This effect was not included in the calculations.

Hinkley, Hansell, Marshall and Harrison (Ceiling Height of 10 m)

A series of experiments was conducted in a building with a space of 53 m × 22 m × 11.3 m high. A 2 m square hexane fire produced an HRR of 4.6 MW. The HRR_c was estimated to be 3.05 MW. The roof was carried on 1 m deep timber beams and a draft curtain 3.2 m deep as measured from the bottom of the beams, divided the building into two spaces. A false level ceiling 10 m above the floor was attached to the bottom of the beams in the space where the experiments were conducted. The data presented by the authors represented the mean taken over the period from 300 s to 600 s after the start of the experiment when the measurements provided relatively steady temperatures. The average of two experiments with no ceiling vents or operating sprinklers is used in the comparison below. These were only two experiments with these conditions reported by the authors. Additional information concerning the experiments can be found in Reference [9].

In modeling this experiment, a square enclosure 21.4 m × 28.7 m with a 10 m high ceiling was used with the fire positioned 0.05 m above the floor. A draft curtain 3.2 m deep and 21.4 m wide was positioned at each end with the other sides being walls. The ceiling material was approximated by glass while the walls were gypsum using the CFAST database. The ceiling material in the experiment was not glass but the glass material from the CFAST database was used since it produced a computed layer temperature that was close to the measured layer temperature.

Shown in Table 1 are comparisons of the estimated plume centerline temperature to the predictions of DNT. The uncertainties for the radial temperature measurements, as provided by the authors, was ±4°C. The uncertainties for the calculations are based on the assumption that the radiative fraction of the fuel varied from 0.25 to 0.40. The calculated values are based on a radiative fraction of 0.34 that was given by the authors. The uncertainty used for the radiative fraction is designed to include the uncertainty in the HRRs, radiative fraction and thermal losses to the ceiling. The calculated upper layer excess temperature was 87°C while the experimental value was estimated to be 90°C.

DNT over-predicts the plume centerline temperature for this experiment. One explanation for this result is that the experiment may not have had enough thermocouples in the plume region to resolve the plume centerline temperature. It was noted that the plume centerline wandered in location and typically was located some distance away from the fire centerline. The plume centerline temperature used in this comparison was extrapolated

Table 4. Hinkley et al., 10 m ceiling height experiment [9].

Radius (m)	Measured (°C)		DNT (°C)		V 3.1 (°C)	
4	109	113 105	114	125 107	183	201 171
6	103	107 99	104	113 97	173	190 161
8	99	103 95	97	106 91	159	175 149
10	96	100 92	92	100 86	143	157 133

from a radial temperature dependence plot that did not include a temperature at the plume centerline. Hence, the plume centerline temperature may have been higher than was actually reported in the experiment.

Table 4 gives the comparison between the ceiling jet temperature predictions of DNT, CFAST V3.1 and the measured values. The values predicted by DNT lie within the combined uncertainty interval. Since the results of this model depend on predicting the plume centerline temperature accurately, this comparison lends support to the supposition that the measured plume centerline temperature for this experiment is low. The ceiling jet temperature predictions of V3.1 are substantially higher than the measured values.

Gott, Lowe, Notarianni and Davis (Ceiling Height of 15 m)

A series of JP-5 pool fires was conducted in a hangar of size 97.8 m × 73.8 m × 15.1 m. The fires were centered under a draft-curtained area 18.3 m × 24.4 m with a ceiling height of 14.9 m. The draft curtain was 3.7 m deep. Three JP-5 pool fire experiments, a 0.61 m^2 0.48 MW fire, a 1.5 m diameter 2.8 MW fire and a 2.5 m diameter 7.7 MW fire, were modeled. Each comparison was made after the fire totally involved the pan and became steady, the plume was approximately aligned with the geometric center of the experiment, and the temperature measurements at the ceiling became reasonably stable. The radiation fraction used in the calculations was obtained using the relationship [16] where D is the pan diameter.

$$\chi_r = 0.35 \times (2.0/D)^{0.6} \tag{13}$$

Additional information concerning these experiments can be found in Reference [1].

In modeling the experiment, a rectangular space 18.3 m × 24.4 m with a ceiling height of 14.9 m was used. The ceiling was flat. The fire was centered and located 0.25 m above the floor. The ceiling was steel 1/8 taken from the CFAST database. A draft curtain 3.7 m deep enclosed the area.

Table 1 gives the comparisons of the plume centerline temperature predictions of DNT with the measured values. DNT predicts the temperature within the uncertainty intervals for the two smaller fires but over-predicts the temperature for the 7.7 MW fire. The HRR for the 7.7 MW fire was determined by a fuel mass loss method rather than direct load cell measurements which, due to fuel evaporation at the end of the experiment, may lead to an overestimation of HRR but there was no way to determine how much of an overestimate is involved in the measurement.

The uncertainty interval for the measurements was obtained by calculating the RMS temperature fluctuations of five measurements over a 20 s period and is equal to $\pm\sigma$. The uncertainty interval for the calculations was determined by varying the HRR by $\pm 15\%$. This uncertainty should include the uncertainty in the radiative fraction as well as the uncertainty in the HRR. The uncertainty in the HRR was not increased for the 7.7 MW fire.

The comparisons of the ceiling jet temperature predictions of DNT and Version 3.1 with the measured values are presented in Table 5. Only the 2.7 MW fire and the 7.7 MW were used in the comparison owing to the small temperature excess in the ceiling jet for the 0.48 MW experiment. The temperature predictions of DNT were within the combined uncertainty interval for the 2.7 MW experiment and for the 3.1 m position in the 7.7 MW experiment. The temperatures at the 6.1 m and 9.1 m positions for the

Table 5. Gott et al 15 m ceiling height experiments [1].

Fire Size (MW	Radius (m)	Measured (°C)		DNT (°C)		V 3.1 (°C)	
2.7	3.1	42	45 39	42	46 37	46	51 39
	6.1	36	41 30	36	42 32	49	55 43
	9.1	24	30 17	33	40 29	48	54 42
7.7	3.1	85	89 81	98	109 87	125	139 110
	6.1	64	69 59	84	93 75	133	148 118
	9.1	56	60 52	76	84 68	130	145 115

7.7 MW fire were under-predicted by DNT. Version 3.1 of CFAST over-predicted all locations for both experiments except for the 3.1 m position of the 2.7 MW fire. The uncertainty intervals for the ceiling jet temperatures were treated in the same manner as for the plume centerline temperatures.

Gott, Lowe, Notarianni and Davis (Ceiling Height of 22 m)

A series of JP-5 and JP-8 pool fires was conducted in a hangar of size 73.8 m × 45.7 m and had a barrel roof which was 22.3 m high at the center and 12.2 m high at the walls. Corrugated steel draft curtains were used to divide the ceiling into five equal bays approximately 14.8 m × 45.7 m with the fire experiments conducted in the middle bay and centered under the 22.3 m high ceiling. Nine experiments with fire sizes ranging from 1.4 MW to 33 MW were modeled. Each comparison was made after the fire totally involved the pan and became steady, the plume was approximately aligned with the geometric center of the experiment and the temperature measurements at the ceiling became reasonably stable. The radiation fraction was calculated using Equation 13 and varied as a function of pan diameter. Additional information concerning these experiments can be found in Reference [1].

In modeling the experiment, a rectangular space 14.8 m × 45.7 m with a ceiling height of 22.3 m was used. The ceiling was flat. The fire was centered and located 0.3 m above the floor. The ceiling was steel 1/8 taken from the CFAST database. Draft curtains 8.9 m deep were attached to the 45.7 m sides and walls bounded the 14.8 m sides.

Table 1 presents the comparison of the plume centerline temperature predictions of DNT with the measured values. The predictions of DNT were within the uncertainty intervals for all the experiments. The uncertainty interval for the measurements was obtained by calculating the RMS temperature fluctuations of five measurements over a 20 s period and is equal to $\pm\sigma$. The uncertainty interval for the calculations was determined by varying the HRR $\pm$ 15%. This uncertainty should include the uncertainty in the radiative fraction as well as the uncertainty in the HRR.

Table 6 presents the comparison of the ceiling jet temperature predictions of DNT and Version 3.1 with the measured values at distances of 6.1 m, 9.1 m, and 12.2 m from plume center. These measurements were along the curved part of a barrel roof. The predictions of DNT were within or slightly above the uncertainty interval for the measured values while the predictions of Version 3.1 were substantially above the measured values. The uncertainty intervals for the ceiling jet temperatures were treated in the same manner as for the plume centerline temperatures.

Table 6. Gott et al. 22 m ceiling height experiments [1].

Fire Size (MW)	Radius (m)	Measured (°C)	DNT (°C)	V 3.1 (°C)
2.8	6.1	22 (24 / 20)	23 (25 / 21)	34 (38 / 30)
	9.1	20 (22 / 18)	21 (23 / 19)	32 (36 / 29)
	12.2	19 (21 / 17)	20 (22 / 18)	31 (35 / 28)
4.9	6.1	32 (33 / 31)	38 (42 / 34)	59 (77 / 52)
	9.1	31 (33 / 29)	34 (38 / 31)	57 (63 / 50)
	12.2	30 (32 / 28)	32 (36 / 29)	55 (62 / 48)
7.9	6.1	53 (55 / 51)	57 (63 / 51)	92 (103 / 81)
	9.1	48 (50 / 46)	52 (56 / 46)	89 (100 / 78)
	12.2	43 (44 / 42)	49 (54 / 43)	87 (98 / 77)
14.3	6.1	84 (91 / 77)	93 (102 / 81)	156 (175 / 138)
	9.1	74 (82 / 66)	85 (94 / 75)	151 (170 / 132)
	12.2	71 (76 / 66)	80 (88 / 70)	147 (165 / 130)
14.6	6.1	85 (92 / 78)	95 (106 / 84)	160 (178 / 140)
	9.1	78 (86 / 70)	87 (97 / 77)	155 (173 / 136)
	12.2	72 (77 / 67)	81 (91 / 72)	151 (169 / 132)
15.7	6.1	88 (91 / 85)	100 (111 / 89)	169 (188 / 144)
	9.1	79 (82 / 76)	92 (102 / 81)	164 (182 / 129)
	12.2	70 (73 / 67)	86 (95 / 76)	160 (178 / 131)
33	6.1	188 (199 / 177)	173 (191 / 151)	300 (326 / 261)
	9.1	164 (172 / 156)	158 (175 / 139)	290 (315 / 253)
	12.2	143 (148 / 138)	148 (164 / 130)	280 (304 / 234)

SUMMARY

New algorithms for the calculation of plume centerline temperature and ceiling jet temperature have been tested in CFAST for a number of experiments with different ceiling heights, draft curtain depths and fuel types. Evans' plume centerline temperature algorithm, implemented in DNT, predicted temperatures which were within the combined uncertainty interval for the measurement and calculation for eleven of the sixteen experiments in which centerline temperatures were measured as shown in Figure 5. In general, the combined uncertainty interval can be taken as equal to ±20%. The maximum error was roughly 25% for all sixteen comparisons. Evans' algorithm over-predicted most of the temperatures. The tendency for this algorithm to over-predict the temperature may be the result of a choice of constants in the plume algorithm or it may result from the layer temperature calculation in CFAST.

The ceiling jet algorithm, DNT, performed extremely well, predicting ceiling jet temperatures within the combined uncertainty interval for eleven of the twelve experimental comparisons as shown in Figure 6. The algorithm gave substantially better predictions than the current algorithm used in Version 3.1 of CFAST that over-predicted the ceiling jet temperature by

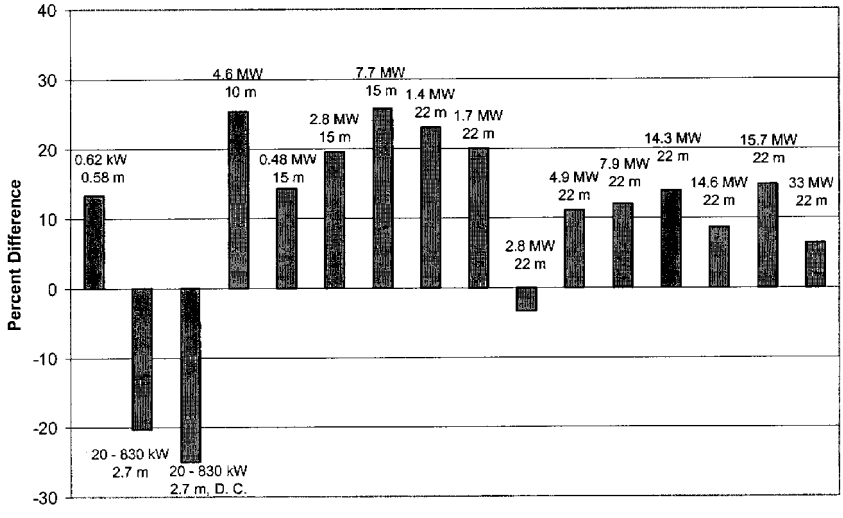

Figure 5. *Percentage difference, prediction minus measurement, for the plume centerline temperature excess for all experiments. For the 2.7 m experiments where comparisons were made based on a growing fire, the percentage difference is the average of all the comparisons.*

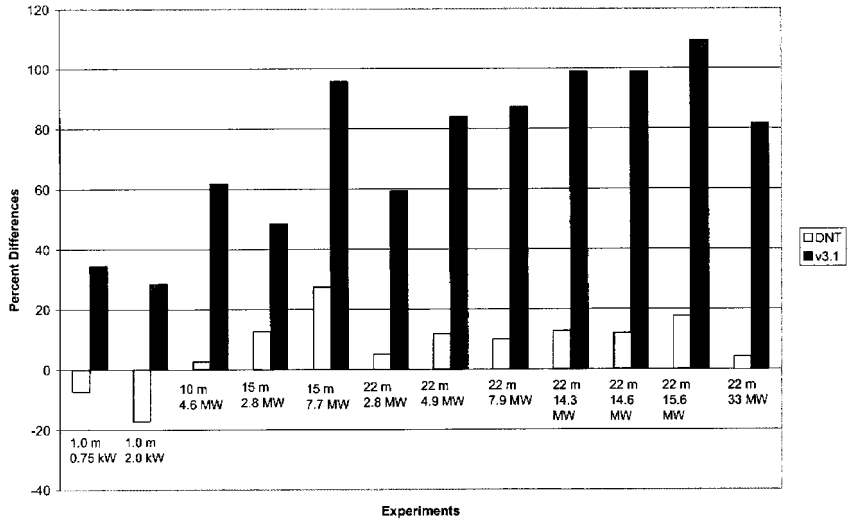

Figure 6. *Percentage difference, prediction minus measurement, for the ceiling jet temperature excess for all experiments. For each experiment, the percentage difference represents the average of the individual percent differences at each radial position. The first bar represents the predictions of DNT and the second bar represents the predictions of CFAST version 3.1.*

20% or more in all twelve experiments. Since the ceiling jet temperature was compared in a number of locations for every experiment, the percent difference given in Figure 6 is based on an average error over the positions of comparison for each experiment.

NOMENCLATURE

c_p	heat capacity of air at constant pressure [J/kg K]
C_T	experimentally determined constant (9.115) [dimensionless]
D	fire diameter [m]
g	acceleration of gravity [m/s^2]
H_1	height of ceiling above the fire surface [m]
H_2	height of ceiling above the substitute fire [m]
Q	heat release rate (HRR) [kW]
Q_c	convective heat release rate (HRR$_c$) [kW]
$Q^*_{I,1}$	strength of fire at the layer interface [dimensionless]
$Q^*_{I,2}$	strength of substitute source at the layer interface [dimensionless]
r	radial distance from plume centerline [m]

r_o radial distance from plume centerline to beginning of ceiling jet [m]
ΔT excess temperature [°C]
ΔT_p excess plume centerline temperature [°C]
T_u upper layer temperature [K]
T_∞ ambient temperature [K]
y_J approximate ceiling jet thickness [m]
y_L layer thickness [m]
z vertical position above the floor [m]
z_o location of the virtual origin above the fire surface [m]
$Z_{I,1}$ height of layer interface above the fire surface [m]
$Z_{I,2}$ height of layer interface above the substitute fire [m]
α experimentally determined constant (0.44) [dimensionless]
β experimentally determined constant (0.9555) [dimensionless]
ξ ratio of upper to lower layer temperature [dimensionless]
ρ_o ambient density of air [kg/m^3]
χ_r radiative fraction [dimensionless]

REFERENCES

1. Gott, J.E., Lowe, D.L., Notarianni, K.A. and Davis, W.D., "Analysis of high bay hangar facilities for detector sensitivity and placement", *National Institute of Standards and Technology*, NIST Technical Note 1423, 1997, pp. 1–315.
2. Davis, W.D., "The zone fire model JET: a model for the prediction of detector activation and gas temperature in the presence of a smoke layer", *National Institute of Standards and Technology*, NISTIR 6324, 1999, pp. 1–51.
3. Davis, W.D. and Cooper, L.Y., "Estimating the environment and the response of sprinkler links in compartment fires with draft curtains and fusible link-actuated vents - Part II: user guide for the computer code LAVENT", *National Institute of Standards and Technology*, NISTIR 89-4122, 1989, pp. 1–36.
4. Peacock, R.D., Reneke, P.A., Jones, W.W., Bukowski, R.W. and Forney, G.P., "A user's guide for FAST: engineering tools for estimating fire growth and smoke transport", *National Institute of Standards and Technology*, Special Publication 921, 1997, pp. 1–180.
5. Evans, D.D., "Calculating sprinkler actuation time in compartments", *Fire Safety Journal*, Vol. 9, 1985, pp. 147–155.
6. Evans, D.D., "Calculating fire plume characteristics in a two layer environment", *Fire Technology*, Vol. 20, No. 3, 1984, pp. 39–63.
7. Motevalli, V. and Ricciuti, C., "Characterization of the confined ceiling jet in the presence of an upper layer in transient and steady-state conditions", *National Institute of Standards and Technology*, NIST-GCR-92-613, 1992, pp. 1–134.
8. Heskestad, G. and Delichatsios, M.A., "Environments of fire detectors - Phase II: effect of ceiling configuration. Volume II. Analysis", *National Institute of Standards and Technology*, NBS-GCR-78-129, 1978, pp. 1–100.
9. Hinkley, P.L., Hansell, G.O., Marshall, N.R. and Harrison, R., "Large-scale experiments with roof vents and sprinklers Part 1: temperature and velocity measurements in immersed ceiling jets compared with a simple model", *Fire Science and Technology*, Vol. 13, No. 1&2, 1993, pp. 19–41.

10. Cooper, L.Y., ''Fire-plume-generated ceiling jet characteristics and convective heat transfer to ceiling and wall surfaces in a two-layer fire environment: uniform temperature ceiling and walls'', *Fire Science and Technology*, Vol. 13, No. 1&2, 1993, pp. 1–17.
11. Morton, B.R., Taylor, B.I. and Turner, J.D., ''Turbulent gravitational convection from maintained and instantaneous sources'', *Proc. Roy. Soc.* A234, 1956, pp. 1–23.
12. Heskestad, G., ''Engineering relations for fire plumes'', *Fire Safety Journal*, Vol. 7, 1984, pp. 25–32.
13. Cooper, L.Y., ''Fire-plume-generated ceiling jet characteristics and convective heat transfer to ceiling and wall surfaces in a two-layer zone-type fire environment'', *National Institute of Standards and Technology*, NISTIR 4705, 1991, pp. 1–32.
14. Zukowski, E.E., Kubota, T. and Cetegen, B., ''Entrainment in fire plumes'', *Fire Safety Journal*, Vol. 3, 1980, pp. 107–121.
15. Heskestad, G. and Delichatsios, M.A., ''The initial convective flow in fire'', *17th International Symposium on Combustion*, Combustion Institute, Pittsburgh, PA, 1978, pp. 1113–1123.
16. Alpert, R.L., ''Calculation of response time of ceiling-mounted fire detectors'', *Fire Technology*, Vol. 8, 1972, pp. 181–195.
17. Davis, W.D., Notarianni, K.A. and Tapper, P.Z., ''An algorithm for calculating the plume centerline temperature and ceiling jet temperature in the presence of a hot upper layer'', *National Institute of Standards and Technology*, NISTIR 6178, 1998, pp. 1–23.
18. Zukowski, E.E. and Kubota, T., ''An experimental investigation of the heat transfer from a buoyant gas plume to a horizontal ceiling, Part II. effects of ceiling layer'', *National Institute of Standards and Technology*, NBA-GCR-77-98, 1975, pp. 1–73.